

Barkhausen noise in soft amorphous magnetic materials under applied stress

Gianfranco Durin¹ and Stefano Zapperi²

¹ *Istituto Elettrotecnico Nazionale Galileo Ferraris and INFM, Corso M. d'Azeglio 42, I-10125 Torino, Italy*

² *PMMH ESPCI, 10 rue Vauquelin, 75231 Paris-Cedex 05, France*

We report experimental measurements of Barkhausen noise on Fe₆₄Co₂₁B₁₅ amorphous alloy under tensile stress. We interpret the scaling behavior of the noise distributions in terms of the depinning transition of the domain walls. We show that stress induced anisotropy enhance the effect of short-range elastic interactions that dominate over long-range dipolar interactions. The universality class is thus different from the one usually observed in Barkhausen noise measurements and is characterized by the exponents $\tau \simeq 1.3$ and $\alpha \simeq 1.5$, for the decay of the distributions of jump sizes and durations.

PACS numbers: 75.60.Ej, 75.60.Ch, 64.60.Lx, 68.35.Ct

I. INTRODUCTION

The Barkhausen effect has received a renewed theoretical interest in the last few years, because of its connections with interface depinning and non-equilibrium critical phenomena. We have recently proposed^{1,2} a microscopic model of the Barkhausen effect based on the dynamics a flexible domain wall on a random environment. The model gives a satisfactory explanation of many of the experimental results reported in literature. In particular, we are able to justify the occurrence of the power law distributions of Barkhausen jumps and compute the critical exponents. In the limit of a vanishing field driving rate, the size distribution scales as $P(s) \sim s^{-\tau} f(s/s_0)$, where $\tau = 3/2$, and the cutoff scales with the demagnetizing factor as $s_0 \sim 1/k$. Similarly, the duration distribution scales as $P(T) \sim T^{-\alpha} g(T/T_0)$, where $\alpha = 2$, and the cutoff scales as $T_0 \sim 1/\sqrt{k}$. These results are the strict consequence of the presence of long-range dipolar interactions and are in perfect agreement with experiments on amorphous alloys and polycrystalline samples³⁻⁵.

In a previously introduced model⁶, based on a description of the domain wall similar to ours, dipolar interactions were ignored, giving rise to different critical exponents $\tau \sim 1.3$, and $\alpha \sim 1.5$. Comparable experimental values have only been reported for Perminvar (30% Fe, 45% Ni, 25% Co)⁶, where $\tau \sim 1.33$. In this paper, we show that the critical exponents in Fe₆₄Co₂₁B₁₅ amorphous alloy under tensile stress display the values $\tau \sim 1.28$, and $\alpha \sim 1.5$, indicating that the experiment is described by short-range interface models. We explain these results noting that for magnetostrictive materials, such as Fe₆₄Co₂₁B₁₅, magneto-elastic interactions enhance the effect of the surface tension over the long-range dipolar forces.

II. THEORY

Before describing in detail the experimental results, we summarize the main theoretical results recently discussed in Refs. 1,2. We consider a single 180° domain wall, described by its position $h(\vec{r})$, dividing two regions of opposite magnetization directed along the x axis. The total energy for a given configuration is the sum of different contributions due to magnetostatic, ferromagnetic and magneto-crystalline interactions, and gives rise to the following equation of motion^{1,2}

$$\frac{\partial h(\vec{r}, t)}{\partial t} = H - k\bar{h} + \nu_0 \nabla^2 h(\vec{r}, t) + \int d^2 r' K(\vec{r} - \vec{r}') (h(\vec{r}') - h(\vec{r})) + \eta(\vec{r}, h), \quad (1)$$

where H is the applied field, k is the demagnetizing factor and $\bar{h} \equiv \int d^2 r' h(\vec{r}', t)/V$, ν_0 is the surface tension of the wall, K is the kernel due to dipolar interactions given by

$$K(\vec{r} - \vec{r}') = \frac{\mu_0 M_s^2}{2\pi |\vec{r} - \vec{r}'|^3} \left(1 + \frac{3(x - x')^2}{|\vec{r} - \vec{r}'|^2} \right), \quad (2)$$

and $\eta(\vec{r}, h)$ is a Gaussian uncorrelated random field taking into account all the possible effects of dislocations, residual stress and non-magnetic inclusions.

When $k = 0$, Eq. (1) displays a depinning transition as a function of the field and the corresponding critical exponents can be obtained with renormalization group methods^{7,8}. For $k > 0$, which corresponds to the experiments we are describing here, the domain wall displays a steady motion *around* the depinning transition⁶. For low driving rates, the velocity of the wall shows avalanches whose distributions are characterized by the scaling laws expected close to the depinning transition.

The upper critical dimension of Eq. (1) is $d_c = 3$ so that the dynamics can be described by a mean-field equation¹. This is the reason of the success of a mean-field phenomenological model⁹ to explain most of the experimental data. In fact, the critical exponents take mean-field values $\tau = 3/2$, and $\alpha = 2$, with a small correction at non-zero driving rates, $\tau = 3/2 - c/2$, and $\alpha = 2 - c$, where c is a dimensionless parameter proportional to the driving rate dH/dt , in agreement with experimental data on many different materials²⁻⁵.

These results change when the long-range kernel (Eq. (2)) is absent and the surface tension is the most relevant term in the equation. The upper critical dimension changes to $d_c = 5$, with critical exponents significantly lower, $\tau = 1.25$, and $\alpha = 1.43$ from renormalization group calculations^{7,8,10}, and $\tau \simeq 1.3$, and $\alpha \simeq 1.5$ from simulations^{10,11}.

III. EXPERIMENTAL RESULTS AND SIMULATIONS

Ribbons of an high magnetostrictive ($\lambda_s = 46.5 \cdot 10^{-6}$) $\text{Fe}_{64}\text{Co}_{21}\text{B}_{15}$ amorphous alloy are prepared by planar flow casting in air. We employ a single strip of 30 cm length under tensile stress from 0 to 140 MPa. The applied stress induces uniaxial anisotropies, radically changing the domain structure. This kind of high magnetostrictive alloy shows a typical behavior of the coercive field H_c (see for instance¹²): a fast decrease of H_c up to a typical stress value $\sigma_0 \sim 10\text{MPa}$, and a roughly linear increase at high stresses. This behavior is due to changes in the domain structure: the quenched-in stresses dominate at low tensile stress, resulting in a complicated pattern of maze domains. As the external stress increases, and the uniaxial anisotropy is induced, a simpler domain structure appears, with a few parallel domains in the direction of the stress¹².

The Barkhausen noise measurements are performed as explained in Ref. 3. The visual inspection of Barkhausen signal reveals the changes induced by the stress in the domain wall dynamics (Fig. 1). The amplitude of the signal increases with the stress, resulting in very short and peaked jumps at high stresses. A better characterization of the Barkhausen jump shape is obtained considering the distributions of the amplitude v , the size s , and the durations T ^{3,13}.

As in previous experiments^{3,13,14}, the amplitude distribution is found to decay as

$$P(v) \sim v^{-(1-c)} \exp(-v/v_0), \quad (3)$$

where c is the normalized driving rate. We show in Fig. 2 that the cutoff v_0 increases with the stress, scaling as $v_0 \sim \sigma^{0.5}$. Size and duration distributions are collected at nearly same the value of $c = 0.1 - 0.2$, showing exponents $\tau \sim 1.28 \pm 0.02$ (Fig. 3), and $\alpha \sim 1.5 \pm 0.1$, *independent* of the applied stress, provided that $\sigma > \sigma_0$. At low applied stress ($\sigma < \sigma_0$), where the domain structure is more complicated and the Barkhausen signal/background noise ratio is reduced, it is difficult to obtain reliable estimates of the exponents.

For $\sigma \simeq \sigma_0$, we also measured the variations of the critical exponents with the parameter c . Unlike mean-field theory⁹, here the dependence from c is quite weak within the fitting error bar, in agreement with the result reported for the Perminvar⁶.

The cutoff of the distributions shows an intriguing behavior: the cutoff of the size distribution s_0 is nearly independent on the stress (Fig. 3), while the duration is progressively reduced with a stress dependence of the type $T_0 \sim \sigma^{-0.5}$. These results quantify the qualitative picture of the signal discussed above: the amplitude of the signal increases with the stress, while avalanche durations are shorter, so that the avalanche sizes roughly do not change with the stress.

In order to understand the experimental results, we perform a serie of simulations of a discretized version of Eq. (1) without the long-range kernel⁶. We employ different field driving rates and evaluate the parameter c using the amplitude distributions. We observe small variations in the critical exponents: $\tau = 1.26 \pm 0.04 - (0.16 \pm 0.05)c$ and $\alpha = 1.40 \pm 0.05 - (0.25 \pm 0.05)c$, in excellent agreement with experiments.

IV. DISCUSSION

The critical exponents of the experimental Barkhausen signal in a magnetostrictive sample under stress are in agreement with the results of our simulations and those previously reported^{6,11}, neglecting dipolar interaction in the equation of motion. This implies that simple domain structures with a few straight domains, spanning from end to

end, as those induced by tensile stress, are well described by the universality class of the equation with elastic surface tension. This observation provides an interesting experimental case where accurate results can be compared with statistical theories of interface depinning.

In general terms, if we believe that Eq. (1) describes all the essential elements of the domain wall dynamics, we expect that the experimental results will belong to either of the two universality classes considered above. In general, it is not easy to predict the universality class from the knowledge of the domain structure of a sample, and its magnetic or thermal treatment. We can, however, estimate the relative weights of the dipolar and elastic energies and obtain a rough classification of the results that can be observed in different materials.

Roughly speaking, the energy associated to the “elastic” tension of the wall is $E_{el} \sim \nu_0 S$, where S is the area of domain wall, while the magnetostatic energy is of the order of $E_{ms} \sim \mu_0 M_s^2 k^* V$, where k^* is the demagnetizing factor associated with the region of volume V where magnetic charges appear¹⁵. As a first approximation, we can take $V = S\delta_w$, where δ_w is the domain wall width. Since $\nu_0 \sim \sqrt{AK}$, and $\delta_w \sim \sqrt{A/K}$, where A is the exchange constant and K the anisotropy constant, the ratio between the two terms is of the order of $r \equiv E_{el}/E_{ms} \sim 10^{-6}K/k^*$, since $\mu_0 M_s \sim 1T$. The factor k^* cannot be easily evaluated, because it depends strongly on the spatial distribution of the charges. It vanishes for a perfectly rigid wall and is of order 1 for a large bending of the wall. In general, considering only a small bending of the surface, we can estimate $k^* \sim 10^{-2}$, which correspond to length/width ratio of the order of 10 or more, giving $r \sim 10^{-4}K$. In soft amorphous alloys as the one we employ in our experiments, the average anisotropy constant $\langle K \rangle$ is of the order of 200 J/m³ (Ref. 12), so that $r \ll 1$, and magnetostatic effects prevail^{2,14}. Under applied stress, the induced anisotropy ($K_\sigma \sim 3/2\lambda_s\sigma$), and the reduced value of k^* , yield $r \geq 1$, so that the surface tension becomes dominant. A similar effect could also explain the experimental results on Perminvar⁶, a material with a low permeability value (~ 250) consistent with a quite high value of $K \sim 10^4 - 10^5$.

In principle, it should be possible to observe the transition between the two universality classes changing the induced anisotropy in an amorphous alloy. Our results do not definitely prove it, since the exponents at low stress have quite large error bars. Experiments on other amorphous alloys are in progress to confirm this hypothesis. Finally, we are currently working to understand quantitatively the scaling of the cutoff of the distributions with the applied stress.

¹ P. Cizeau, S. Zapperi, G. Durin, and H. E. Stanley, Phys. Rev. Lett. **79**, 4669 (1997).

² S. Zapperi, P. Cizeau, G. Durin, and H. E. Stanley, to appear on Phys. Rev. B sept. 1st. 1998.

³ G. Durin, G. Bertotti, and A. Magni, Fractals **3**, 351 (1995).

⁴ G. Durin, in *Proc. of the 14th Int. Conf. on Noise in Physical Systems and 1/f Fluctuations*, C. Claeys and E. Simoen eds. (World Scientific, Singapore, 1997).

⁵ Mean-field exponents are also found in the amorphous alloy Fe₇₃Co₂₁B₁₅ annealed under stress, and in the as-cast Fe₂₁Co₆₄B₁₅. G. Durin, S. Zapperi, in preparation.

⁶ J. S. Urbach, R. C. Madison, and J. T. Markert, Phys. Rev. Lett. **75**, 276 (1995).

⁷ T. Nattermann, S. Stepanow, L. H. Tang, and H. Leschhorn J. Phys. II (France) **2**, 1483 (1992).

⁸ O. Narayan and D. S. Fisher, Phys. Rev. B **48**, 7030 (1993).

⁹ B. Alessandro, C. Beatrice, G. Bertotti, and A. Montorsi J. Appl. Phys. **68**, 2901 (1990); *ibid.* **68**, 2908 (1990).

¹⁰ H. Leschhorn, T. Nattermann, S. Stepanow, and L. H. Tang, Ann. Physik **6**, 1 (1997).

¹¹ M. Bahiana, B. Koiler, S. L. A. De Queiroz, J. C. Denardin and R. L. Sommer, preprint cond-mat/9808017.

¹² C. Appino, G. Durin, V. Basso, C. Beatrice, M. Pasquale, and G. Bertotti, this conference.

¹³ G. Bertotti, G. Durin, and A. Magni, J. Appl. Phys. **75**, 5490 (1994).

¹⁴ G. Durin, P. Cizeau, S. Zapperi, and H. E. Stanley, J. Phys. IV (France) **8**, 319 (1998).

¹⁵ For a detailed discussion of this topic, see for instance: G. Bertotti, *Hysteresis in magnetism* (Academic Press, San Diego, 1998), p. 357ss.

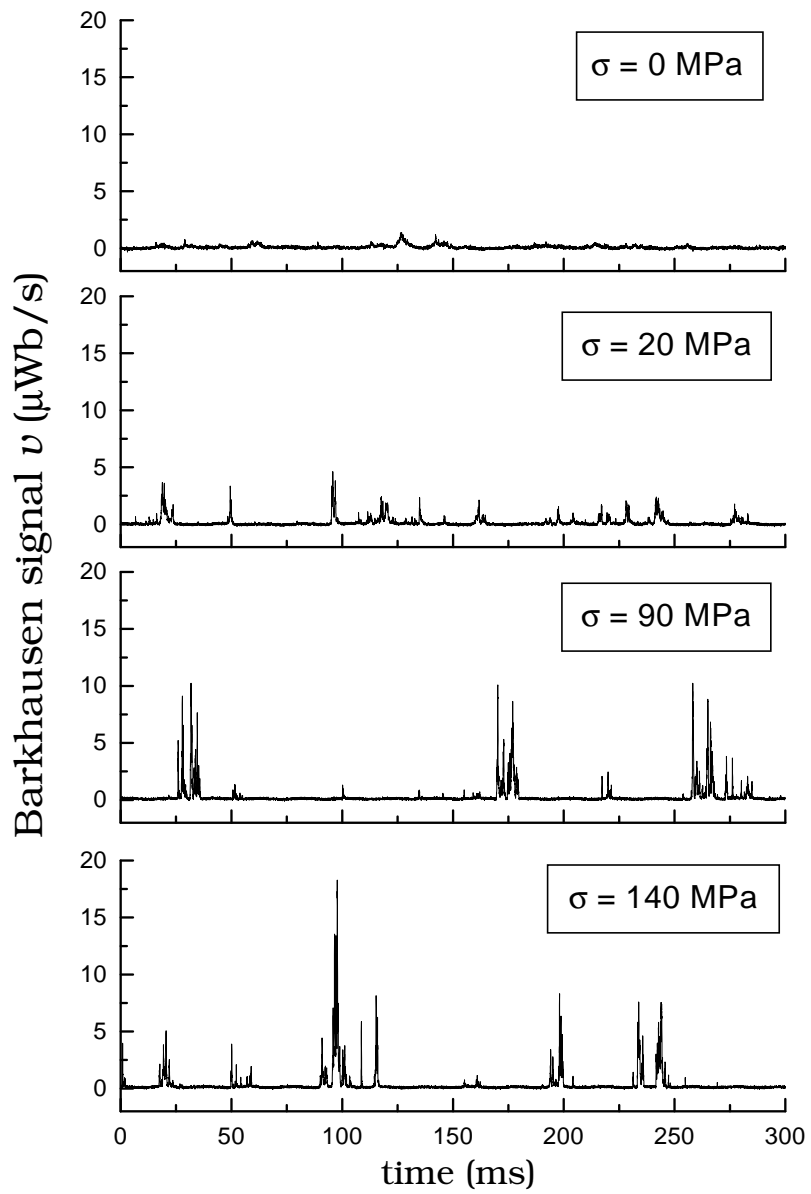


FIG. 1. Barkhausen signal v at different tensile stresses for the as-cast $\text{Fe}_{64}\text{Co}_{21}\text{B}_{15}$ amorphous alloy.

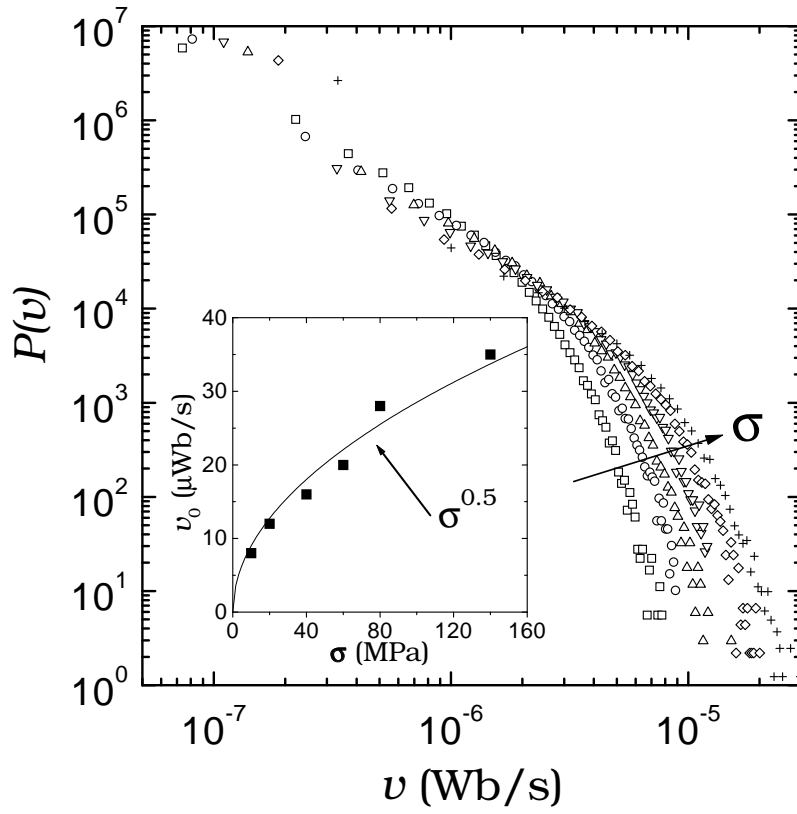


FIG. 2. Distribution of the Barkhausen signal amplitude v at different tensile stresses ($\sigma = 10\text{-}140$ MPa). Data follows the distribution $P(v) \sim v^{-(1-c)} \exp(-v/v_0)$, where c is the normalized driving rate. (Inset) Dependence of the cutoff v_0 on the applied stress, showing $v_0 \sim \sigma^{0.5}$.

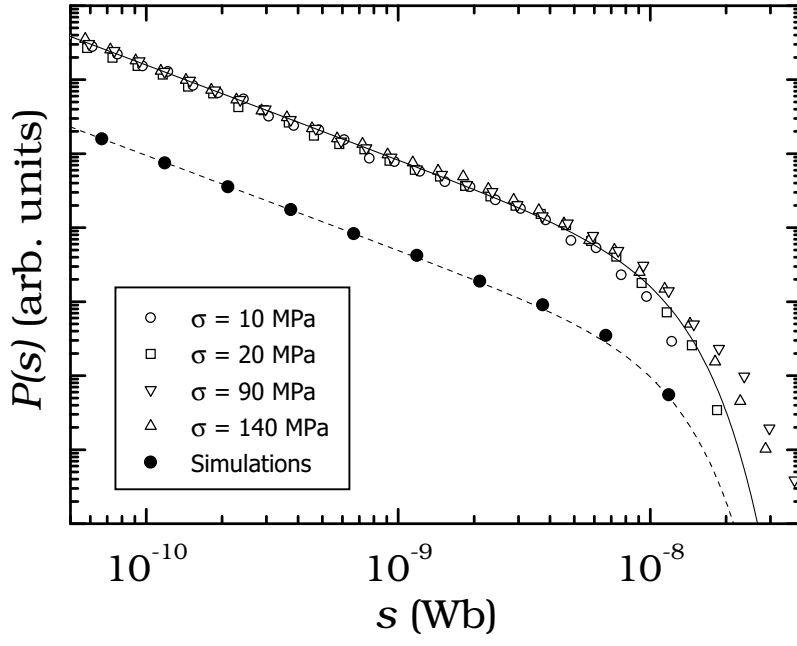


FIG. 3. Experimental size distributions of Barkhausen jumps at different tensile stresses (open dots), compared to the data (solid dots) simulated using Eq. (1) without dipolar interactions. All data are fitted using $P(s) \sim s^{-\tau} \exp(-(s/s_0)^2)$, where $\tau = 1.26$ (experiments), and $\tau = 1.28$ (simulations), with $s_0 \sim 10^{-8}$ Wb. Simulated data are rescaled for comparison.